Asymmetric nuclear matter equation of state

I. Bombaci* and U. Lombardo†
Dipartimento di Fisica, Università di Catania, Corso Italia 57, Catania, Italy
and Istituto Nazionale di Fisica Nucleare, Sezione di Catania, Corso Italia 57, I-95129 Catania, Italy
(Received 25 June 1991)

Systematic calculations of asymmetric nuclear matter have been performed in the framework of the Brueckner-Bethe-Goldstone approach in a wide range of both density and asymmetry parameter. The empirical parabolic law fulfilled by the binding energy per nucleon is confirmed by the present results in all the range of the asymmetry parameter values. The predominant role of the $^3S_1$-$^3D_1$ component of the *NN* interaction is elucidated. A linear variation of the proton and neutron single-particle potentials is found as increasing the neutron excess; a deviation from the phenomenological potentials occurs for highly asymmetric matter as an effect of the self-consistency. The present calculations of the incompressibility predict a strong softening of the equation of state going from symmetric to asymmetric nuclear matter. The proton fraction in equilibrium with neutron matter has been determined from the beta-stability condition and its relevance to the superfluidity of neutron stars has been investigated.

I. INTRODUCTION

Supernova explosions and neutron stars provide us with a unique laboratory where the equation of state (EOS) of nuclear matter can be fruitfully investigated. The prompt shock invoked to understand the explosion mechanism of a type-II supernova requires the EOS to be relatively soft [1]. This is in agreement with the description of the breathing mode in heavy nuclei from which a incompressibility around 210 ± 30 MeV is extracted [2]. According to the model of prompt explosion [3], an electron-capture process drives the star, in the latest stage of collapse, to an equilibrium state where the proton concentration is $Z/A=0.31-0.33$; this gives an incompressibility much lower than in symmetric nuclear matter. On the other hand, systematic analysis of the observed masses of neutron stars [4] favors a stiff EOS. In addition, the sideward flows detected in heavy-ion collisions can be explained by assuming again a stiff EOS with an incompressibility of ~ 400 MeV [5]. However, a momentum-dependent mean field could interpret the same data with a soft EOS [6] as well.

Neutron stars have also attracted much interest because they offer a good chance of studying the occurrence of superfluidity in nuclear matter [7]. This phenomenon is in fact a good candidate to explain the anomalously large relaxation times of the glitches following a neutron-star quake [8]. In particular, an important contribution to the superfluidity could come from the proton fraction in equilibrium with neutrons and electrons in the inner crust of a neutron star [9].

In all these topics an asymmetric nuclear matter is involved and its properties play a crucial role. In fact, the EOS of asymmetric nuclear matter exhibits a minimum which disappears before the pure neutron matter is reached, and thus we expect that the incompressibility decreases and vanishes before the proton fraction vanishes. The equilibrium between neutrons, protons, and electrons in the inner crust of a neutron star is reached at the minimum of the total energy. In this state the proton fraction is controlled by the symmetry energy corresponding to a given baryon density. Thus we can determine the range of neutron density where proton superfluidity occurs inside a neutron star. Despite the interest just outlined, there are only a few calculations of asymmetric nuclear matter based on a microscopic theory. Besides the calculations performed in the nonrelativistic Brueckner [10] and variational approaches [11], a work based on the Dirac-Brueckner approach [12] and one based on the chiral sigma model [13] have to be quoted.

Generally, the asymmetric nuclear matter properties are extracted by interpolating the two extreme situations of symmetric and pure neutron matter with the empirical parabolic approximation [14,15]. This procedure is expected to work well only at low values of the asymmetry parameter $\beta=(N-Z)/A$, which are typical of finite nuclei. The validity of the empirical parabolic law can be checked only by extending the calculations to all the range of β and for many different baryon densities.

In this paper we present such systematic calculations based on the self-consistent Brueckner-Hartree-Fock (BHF) approximation [16] to the Bethe-Goldstone theory. It is well known that this approach does not reproduce the correct saturation point of nuclear matter with only the inclusion of the two-body interaction. But our attention is mainly focused on how nuclear matter properties change in terms of the asymmetry ratio, and some caution has to be taken whenever saturation properties are involved. Nevertheless, the BHF approach offers the advantage of providing a clear understanding of the effect of the different isotopic spin components of the bare *NN* interaction on both the total binding energy and single-particle spectrum. In addition, it gives a simple microscopic justification of the empirical laws governing asymmetric nuclear matter.

The paper is organized as follows. In Sec. II the formalism of the BHF approach is sketched with particular emphasis to the peculiarities of the asymmetry. Section III is devoted to the presentation and discussion of the results obtained from the calculation of binding energy, asymmetry energy, neutron and proton mean fields, and neutron and proton effective masses. In Sec. IV we discuss incompressibility as a function of the asymmetry parameter and its connections with the models of the supernova explosions. In Sec. V the beta-stability condition is investigated in terms of the proton fraction in a neutron star. In Sec. VI some conclusions are drawn.

II. FORMALISM

Our calculations are based on the BHF approach extended to asymmetric nuclear matter. Considerable simplification is achieved in the self-consistent iterative procedure when using separable versions of the realistic *NN* interaction [17]. It has been shown that they are able to reproduce the same results as the original versions [18]. In momentum space a separable *NN* interaction is written in the form

$$v_{\alpha LL'}(q,q')=\sum_{i,j}^{N_\alpha} g_{Li}^{\alpha}(q)\Lambda_{\alpha,ij}g_{L'i}^{\alpha}(q') \ , \tag{1}$$

where $\alpha\equiv(JST)$ specifies the total angular momentum, spin, and isospin of the two interacting nucleons for a given channel; L and L' are the orbital angular momenta of the partial-wave decomposition. The indices i and j run over the rank N_α of the expansion for each channel α. The functions g are the form factors, and the matrix $\Lambda_{\alpha,ij}$ characterizes the interaction strengths. The simplification consists in that the Bethe-Goldstone equation for the G matrix can be worked out in an algebraic way in momentum space. We are left with the G matrix which can be written like the interaction in a separable form

$$G_{\alpha LL'}^{\tau\tau'}(q,q',P,z)=\sum_{i,j}^{N_\alpha} g_{Li}^{\alpha}(q)\Gamma_{\alpha,ij}^{\tau\tau'}(P,z)g_{L'i}^{\alpha}(q') \ , \tag{2}$$

where τ and τ' are the isospin quantum numbers and Γ plays the role of an effective strength defined as

$$[\Gamma_{\alpha,ij}^{\tau\tau'}(P,z)]^{-1}=\Lambda_{\alpha,ij}-\sum_{i,j}^{N_\alpha}\int\frac{q^2dq}{16\pi^2}\frac{g_{Li}^{\alpha}(q)g_{L'i}^{\alpha}(q)Q^{\tau\tau'}(q,P)}{z-e_\tau(q,P)-e_{\tau'}(q,P)} \ . \tag{3}$$

The quantity $e_\tau=\hbar^2k^2/(2m)+U_\tau(k)$ is the single-particle energy of a proton (e_p) or a neutron (e_n). $Q^{\tau\tau'}$ is the angle-averaged Pauli operator. For a given density of protons and neutrons ($k_F^{(\tau)}<k_F^{(\tau')}$), the Pauli operator is

$$Q^{\tau\tau'}=\begin{cases}1 \ \text{if} \ \xi_\tau>1, \ \xi_{\tau'}>1 \ , \\ (\xi_{\tau'}+1)/2 \ \text{if} \ \xi_\tau>1, \ \xi_{\tau'}<1 \ , \\ (\xi_{\tau'}+\xi_\tau)/2 \ \text{if} \ \xi_\tau<1, \ \xi_{\tau'}<1 \ , \\ 0 \ \text{otherwise} \ ,\end{cases} \tag{4}$$

where

$$\xi_\tau=\frac{P^2/4+q^2-(k_F^{(\tau)})^2}{Pq} \ ,$$

and $k_F^{(p)}$ and $k_F^{(n)}$ are the proton and neutron Fermi momenta. In all previous formulas q and P are relative and total momenta, respectively, of the two interacting particles. In the standard BHF procedure the G matrix is self-consistently evaluated with the mean field

$$U_\tau(k)=\sum_{\sigma'\tau'}\sum_{h'}\langle k\sigma\tau;h'\sigma'\tau'|G(e_\tau(k)+e_{\tau'}(h'))|k\sigma\tau;h'\sigma'\tau'\rangle_A \ . \tag{5}$$

The continuous choice [19] has been adopted for the auxiliary potential according to the expectation that higher-order correlations are included at the level two hole-line truncation of the hole-line expansion for the binding energy [20,21]. The present calculations have been carried out by using a separable form of the Paris potential [22], which includes all the following channels: $^1S_0$, $^3P_0$, $^3P_1$, $^3P_2$-$^3F_2$, and $^1D_2$, with $T=1$, and $^3S_1$-$^3D_1$, $^1P_1$, and $^3D_2$, with $T=0$. All calculations have been made in momentum space, and a momentum grid $k_i=0.0(0.1)5.0$ fm^{-1} has been used. Four iterations have been enough to reach convergence in the iterative procedure.

III. RESULTS

A. Binding energy

In Table I most of the results are collected for the binding energy per nucleon $B(\rho,\beta)$ calculated to the lowest order in the hole-line expansion. It is well known that a

TABLE I. Self-consistent results for the binding energy per nucleon versus density $\rho(\mathrm{fm}^{-3})$ and asymmetry parameter β (first column).

	0.038	0.076	0.11	0.14	0.17	0.20	0.30	0.40
0.0	−8.54	−11.55	−13.71	−15.29	−16.48	−17.36	−18.32	−17.01
0.2	−7.75	−10.69	−12.68	−14.12	−15.18	−15.97	−16.66	−15.03
0.4	−5.94	−8.26	−9.85	−10.88	−11.62	−12.02	−11.72	−9.16
0.6	−3.17	−4.45	−5.08	−5.50	−5.68	−5.57	−3.62	0.64
1.0	5.65	8.15	10.06	11.69	13.37	15.21	22.42	31.26

quadratic dependence of the binding energy upon the asymmetry parameter β,

$$B(\rho,\beta)=B(\rho,0)+E_{\mathrm{sym}}(\rho)\beta^2 , \tag{6}$$

has to be expected as in the Fermi-gas model and, in fact, it is experimentally very well confirmed at least for small β. Our results confirm the validity of such an empirical parabolic law, but it is surprising that it is fulfilled up to high values of β. The good quality of such a fit is illustrated in Fig. 1 for some values of the nucleon density ρ. In order to get a deeper understanding of this feature, we have split the total-energy potential into the contribution due to the isospin-zero channels which are active in the proton-neutron interaction and the contribution due to the isospin-one channels which are also present in the proton-proton and neutron-neutron interaction. The result for the saturation density $[\rho_0(0)=0.17\ \mathrm{fm}^{-3}]$ is plotted in Fig. 2. We recognize that the β dependence in the binding energy has to be mostly ascribed to the $T=0$ components, whereas the $T=1$ components are almost equal to those of symmetric nuclear matter at the same density. Moreover, it has been found that of the three $T=0$ channels included in the calculations, the $^1P_1$ and $^3D_2$ contributions cancel out each other for all β values, so that the $T=0$ potential energy plotted in Fig. 2 (solid line) takes contribution mainly from the $^3S_1$-$^3D_1$ channel (small circles). The slow deviation of the $T=1$ contribution from the constant symmetric matter value is due to the dispersive effect of the total mean field and to the reduction of the Pauli principle effect on the scattering between neutrons and protons in the $T=1$ channels.

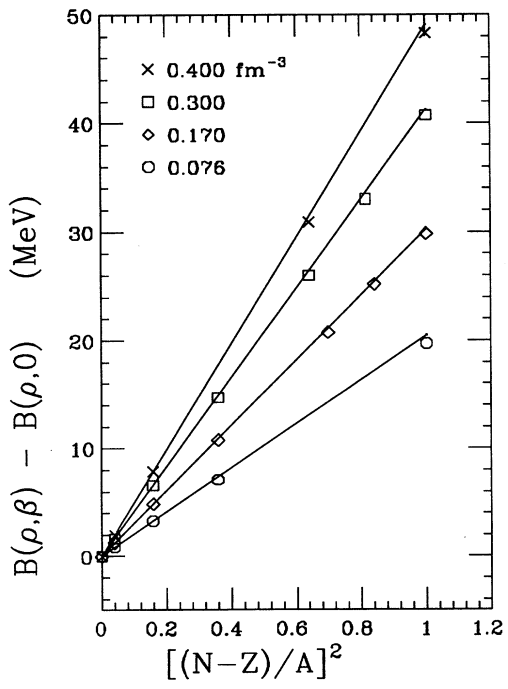

FIG. 1. Total binding energies per nucleon in the range $0\le\beta^2\le1$ at four densities as obtained from the self-consistent calculation. These results are compared with the parabolic fits (straight lines) obtained from the first three values of β (=0.0,0.2,0.4). The slope of each line gives the corresponding symmetry energy.

B. Symmetry energy

The symmetry energy is defined as

$$E_{\mathrm{sym}}(\rho)=\frac{1}{2}\left.\frac{\partial^2 B(\rho,\beta)}{\partial\beta^2}\right|_{\beta=0} . \tag{7a}$$

Assuming the parabolic form for the binding energy per nucleon [Eq. (6)], E_{sym} can be simply evaluated from the

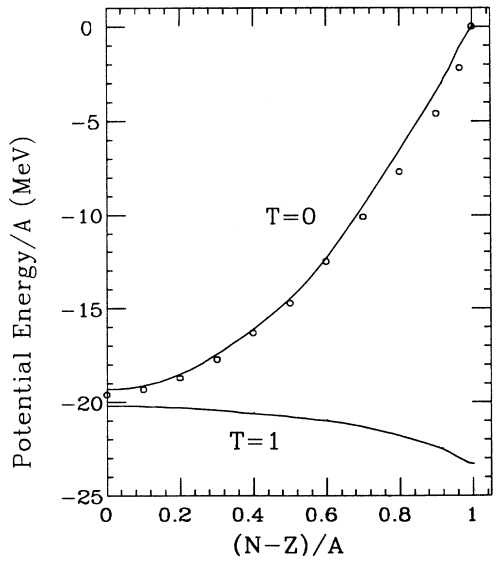

FIG. 2. Splitting of the potential energy per nucleon into the two isospin components vs the asymmetry parameter for the saturation density (0.17 fm^{-3}). The open circles represent the $^3S_1$-$^3D_1$ contribution.

two extreme cases of both pure neutron matter and symmetric nuclear matter according to

$$E_{\rm sym}(\rho)=B(\rho,1)-B(\rho,0)\ . \tag{7b}$$

In view of the results shown in Fig. 1, the estimate based on the last equation gives the same $E_{\rm sym}$ as the numerical fit required by Eq. (7a). Through Eq. (7b), it easy to see that the predominant contribution to $E_{\rm sym}$ comes from the $T=0$ channels (mainly the S-D one). Indeed, the $T=1$ channels give a contribution to the binding energy nearly constant versus β, and then they cancel out in the expression of $E_{\rm sym}$.

Equation (7b) clearly indicates the role of the $^3S_1$-$^3D_1$ channel contribution to the binding energy as increasing β (see Fig. 2), which is maximum in $B(\rho,0)$ and vanishes in $B(\rho,1)$. For the S-D channel the influence of the tensor force is the largest compared to all other channels. Therefore, we can conclude that the symmetry energy is essentially ruled by the tensor component of the NN interaction. From a systematic parabolic fit over three values of β ($\beta=0.0,0.2,0.4$) in the range of densities here considered, we have extracted the symmetry energy, whose numerical values versus density are plotted in Fig. 3 (solid line). For comparison reported also are some recent results obtained in different contexts by assuming *a priori* the parabolic form for $B(\rho,\beta)$. The value at the saturation density is in good agreement with the empirical one of $\sim$28.1 MeV taken from the mass formula [23]. The difference at low densities between our curve and the one of Ref. [14], which uses the same Paris NN interaction, is due to the discrepancy between the two calculations in the channel $^3S_1$-$^3D_1$ (Ref. [18]). Its effect becomes less and less important as the asymmetry increases up to $\beta=1$, where it is no longer active.

The BHF results deviate mainly at high density from the variational results obtained with either the AV14 interaction (dotted curve) and UV14 (dot-dashed curve) [15]. The difference between the two variational predictions can be easily explained as an effect of the different tensor components present in the two interactions. The disagreement between our BHF result and the variational result with the Argonne $v14$ potential cannot be attributed to the two different interactions because Paris and Argonne potentials have been proven to be essentially equivalent in many-body nuclear calculations [21,24].

For high-density values ($\rho>4\rho_0$), the symmetry energy strongly depends on the three-body force, but its effect is too much model dependent to draw any reliable conclusion, as the results of Ref. [15] show. However, this effect on $E_{\rm sym}$ is less and less important for the low densities ($\rho<0.4$ fm^{-3}) we are considering. The uncertainties of the high-density behavior of the symmetry energy become more striking when looking at the results obtained in relativistic approaches [12,13]. In fact, their $E_{\rm sym}$ does not exhibit any saturation at high density, at variance with nonrelativistic calculations [15].

C. Single-particle spectrum

Neutron and proton single-particle potentials have been simultaneously and self-consistently calculated together with their corresponding effective interactions, i.e., G matrices. The results at two densities are reported in Fig. 4. The effect of asymmetry can be clarified by splitting neutron and proton mean fields into their components in such a way as to single out explicitly the dependence on the respective phase space:

$$U_p=U_{pp}+U_{pn}=\tfrac{1}{2}\rho(1-\beta)u_{pp}+\tfrac{1}{2}\rho(1+\beta)u_{pn}\ , \tag{8}$$

$$U_n=U_{nn}+U_{np}=\tfrac{1}{2}\rho(1+\beta)u_{nn}+\tfrac{1}{2}\rho(1-\beta)u_{np}\ , \tag{9}$$

where the $u_{\tau\tau'}$ are the average effective interaction in the phase space. In Fig. 5 the value at $k=0$ of the single-particle potential is plotted versus the asymmetry param-

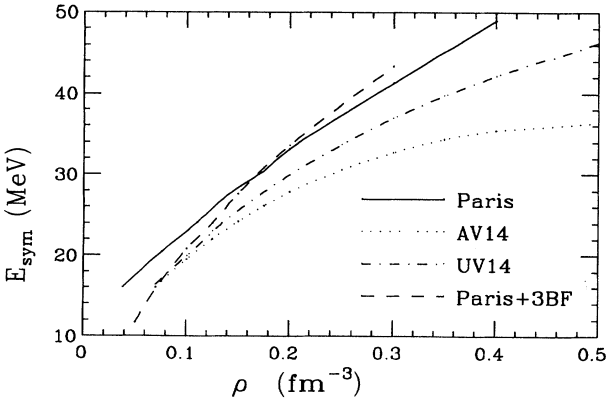

FIG. 3. Symmetry energy versus density from the parabolic fits (solid curve) in comparison with the results of Ref. [14] (dashed curve) and Ref. [15] (dotted and dot-dashed curves).

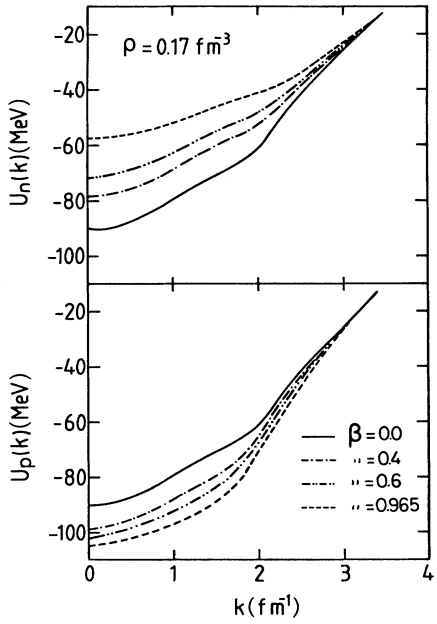

FIG. 4. Self-consistent (a) neutron potential U_n and (b) proton potential U_p for different asymmetry parameters.

eter for two densities. U_{pp} and U_{np} are the mean fields felt, respectively, by proton and neutron in the proton background, which, as expected, vanish at $\beta=1$. U_{nn} and U_{pn} are the same fields generated by the neutron background. The larger variation of U_{pn} is an effect of the $T=0$ channels of the interaction that is, of course, missing in U_{nn}.

The variation of proton and neutron potentials is linear and almost symmetric with respect to their common value at $\beta=0$ for small β. This supports the validity of the Lane potential [25], which has been applied to the nuclear scattering processes. A similar feature is observed in the experimental proton and neutron Fermi energies recently calculated [26] from the $(A+1)$ and A nucleon systems in the range $0.0<\beta<0.24$. The neutron Fermi energy linearly increases and the proton Fermi energy, suitably corrected by the Coulomb energy, linearly decreases, in nice agreement with our results. The slopes evaluated in Ref. [26] are 31.3 and -57.5 MeV for the neutron and proton Fermi energies, respectively, while we obtain 57.3 and -58.9 MeV for the same quantities. However, the inclusion of the single-particle correlations due to the rearrangement term in the mass operator expansion [17] decreases the value of the slope for the neutron Fermi energy, giving a better agreement with the fit of the experimental data reported in Ref. [26].

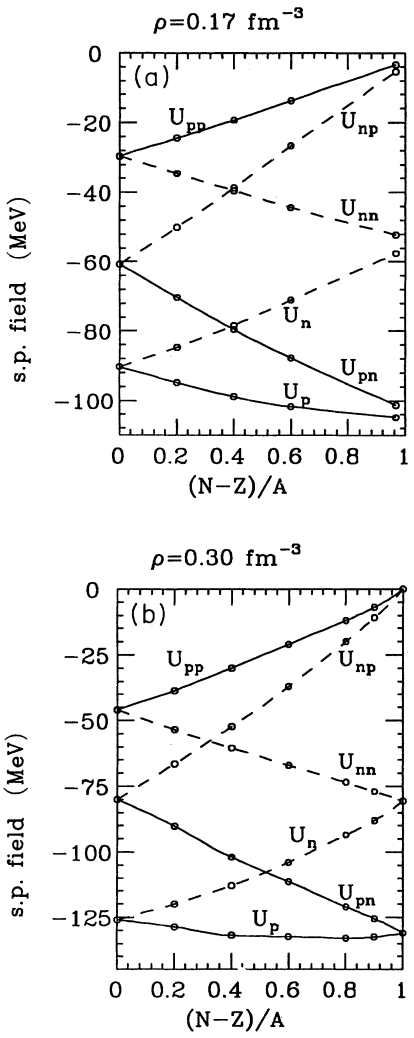

FIG. 5. Proton and neutron potentials at $k=0$ versus asymmetry parameter for (a) $\rho=0.17$ fm^{-3} and (b) $\rho=0.3$ fm^{-3}. The curve indicated by U_p is the sum of U_{pp} and U_{pn}; the curve indicated by U_n is the sum of U_{nn} and U_{np}.

Symmetric variation would mean that $u_{pp}=u_{nn}$ and $u_{pn}=u_{np}$, but we find a significant deviation, as can be seen in Fig. 5, at higher β. For $\rho=0.17$ fm^{-3} the deviation from a symmetric behavior of the neutron and proton potentials is a slowly increasing function of β, reaching at $\beta=1$ a value of ~ 17 MeV, while the difference $\Delta U=U_n-U_p$ is ~ 47 MeV in pure neutron matter. Thus some caution has to be taken when extending to highly asymmetric matter the application of phenomenological interactions such as Skyrme that assume symmetric variation of neutron and proton mean fields.

Another quantity which characterizes the single-particle potential is the effective mass evaluated from the slope of U at the Fermi momentum,

$$\frac{m_\tau^*}{m}=\left[1+\frac{m}{\hbar^2 k}\frac{dU_\tau}{dk}\right]^{-1}_{k=k_F^{(\tau)}}, \tag{10}$$

whose numerical values are reported in Fig. 6. As expected, the above-mentioned deviation occurs also in this quantity. The linear dependence of the single-particle potential on the asymmetry parameter is consistent with the β^2 law fulfilled by the binding energy and can be interpreted as a bulk effect of the gradual reduction of the phase space of protons as β increases. On the other hand, the shift from symmetric variation observed in either the proton and neutron potentials and effective mass has to be attributed to the self-consistent treatment of the G matrix, which determines the effective NN interaction and the mean fields in the BHF approach.

IV. INCOMPRESSIBILITY

The basic physical inputs for describing the iron-core collapse of a presupernova, using hydrodynamical models, are the initial mass of the iron core and nuclear equation of state (EOS). The role of the nuclear EOS for the

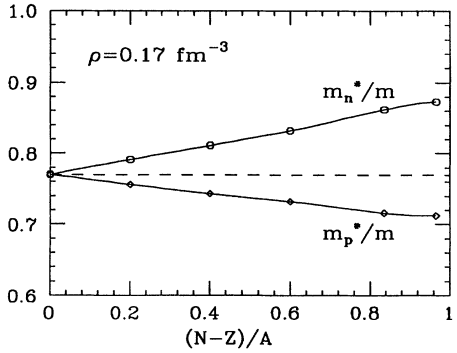

FIG. 6. Proton and neutron effective masses [Eq. (10)] versus β for density equal to 0.17 fm^{-3}.

success of the prompt explosion mechanism has been recently investigated by Baron, Cooperstein, and Kahana (BCK) [1,3]. To solve the hydrodynamic equations, BCK used the following phenomenological EOS:

$$P(\rho)=\frac{K_0(\beta)}{9\gamma}\rho_0(\beta)\left[\left[\frac{\rho}{\rho_0(\beta)}\right]^{\gamma}-1\right], \tag{11}$$

where $\rho_0(\beta)$ and $K_0(\beta)=K_0(\rho_0(\beta))$ are the saturation density and the incompressibility modulus at saturation with an asymmetry parameter β. They used the commonly accepted value [2]

$$K_0(0)=210\pm30 \text{ MeV},$$

for symmetrical nuclear matter, taking the high-density adiabatic index γ in the range 2–3.

Because of the neutrino trapping, neutron-rich asymmetric matter is formed during the collapse of the iron core, and the asymmetry parameter β stays almost constant ($\beta\sim\frac{1}{3}$) for all the collapsing time (up to the core rebound and shock wave formation). Therefore the properties of asymmetric nuclear matter with $\beta\sim\frac{1}{3}$ affect the EOS [Eq. (11)] by producing a decrease in the incompressibility,

$$K_0(\beta)=9\rho_0^2(\beta)\frac{d^2}{d\rho^2}B(\rho,\beta)|_{\rho_0(\beta)},$$

and in the saturation point density $\rho_0(\beta)$ with respect to the symmetrical case. The authors of Ref. [1] found that this softening of the EOS plays a crucial role in generating prompt explosion for stars in the mass range $(12-15)M_\odot$ (where $M_\odot=10^{33}$ g is the mass of the Sun).

In their calculations the dependence upon the asymmetry parameter was described by the relations

$$K_0(\beta)=K_0(0)(1-a\beta^2), \tag{12}$$

$$\rho_0(\beta)=\rho_0(0)(1-b\beta^2), \tag{13}$$

with $a=2.0$ and $b=0.75$. The above-quoted values of the parameters a and b are a fit of the results obtained in Ref. [27] using the Skyrme SkM* force, for which $K_0(0)=216.6$ MeV.

The dependence upon the asymmetry parameter β of the nuclear matter incompressibility $K_0(\beta)$ has been inadequately investigated.

So far, one of the most sophisticated investigation of the β dependence of K_0 and ρ_0 remains that of Kolehmainen *et al.* [27] using Skyrme-type interactions in the framework of an extended Thomas-Fermi approach. The authors of Ref. [27] found that $K_0(\beta)$ and $\rho_0(\beta)$ strongly change when different Skyrme-type interactions are used in the calculations. Nevertheless the parabolic approximations Eqs. (12) and (13) for low-β values ($\beta\lesssim0.4$) are valid for all cases considered in Ref. [27].

TABLE II. Incompressibility of asymmetric nuclear matter, saturation density, and biding energy per nucleon corresponding to three different values of the asymmetry parameter.

β	K_0 (MeV)	ρ_0 (fm^{-3})	B_0 (MeV)
0.0	182±9	0.288±0.004	−18.35
0.2	174±6	0.277±0.003	−16.74
0.4	124±9	0.237±0.002	−12.19

In view of what we said earlier, one can realize that a microscopic evaluation of the β dependence of K_0 and ρ_0 is very important.

Using the BHF values for the binding energy $B(\rho,\beta)$ (see Table I, keeping β constant, we have fitted $B(\rho)$ by means of a least-squares polynomial fit, from which the K_0 and ρ_0 values listed in Table II have been extracted. The method is quite sensitive to the degree of the polynomial used for the fit. This is reflected in the uncertainty ΔK_0 for the incompressibility modulus, which is in all cases no more than 4–7 %.

Using Eq. (12), our calculated values of $K_0(\beta)$, for low β ($=0.0,0.2,0.4$), can be fitted very well, giving $a=2.027$, $K_0(0)=185$ MeV, and $K_0(\frac{1}{3})=143$ MeV. A comparison is made in Table III between our results and those of Ref. [27]. Our results resemble mainly those relative to the SkM* force of Ref. [27].

The softening of the nuclear matter EOS has been also investigated by Wiringa, Fiks, and Fabrocini [15] for different interactions. They use a variational method with correlation operators, but their results for the asymmetric nuclear matter are not fully microscopic in the sense that they are an interpolation to an arbitrary asymmetry β obtained for the two extreme cases $\beta=0$ (symmetric nuclear matter) and $\beta=1$ (pure neutron matter). Using the values of $K_0(\frac{1}{3})$ computed by Wiringa, Fiks, and Fabrocini [15], we can extract the coefficient a for the parabolic fit of $K_0(\beta)$. This is shown in Table III for the AV14 ±UVII and UV14 + UVII N-N interactions. As we can see, our results for the coefficient a are in a very good agreement with those of Ref. [15]. It is, however, worthy of note that the coefficient a in Eq. (12) is very sensitive to the small uncertainty ΔK_0 we have in the incompressibility modulus. In fact, using the values $K_0(\beta)\pm\Delta K_0$ ($\beta=0.0,0.2,0.4$), we obtain values of a

TABLE III. Parameters of Eq. (12) extracted from a parabolic best fit of the incompressibility of nuclear matter. The result of the present work is compared with the values obtained in different contexts (see text for references).

	Paris	SkM*	SI′	SIII	AV14+UVII	UV14 + UVII
$K_0(0)$	185	216.6	370.3	355.3	209	202
a	2.027	1.988	1.272	1.275	2.196	2.049
$K_0(\frac{1}{3})$	143.3	168.7	318.0	305.0	158	156

which can vary in the range 1.481–2.519. Therefore, a can be evaluated with an uncertainty of about 50%. We believe that a similar uncertainty occurs when the coefficient a is evaluated with the preceding quoted methods [15,27].

Using the values listed in Table II, we have also calculated the parameters $\rho_0(0)$ and b of Eq. (13), which define the low-density change in the saturation density with the asymmetry parameter β. We found $\rho_0(0)=0.289$ and $b=1.115\pm0.083$.

V. BETA-STABLE MATTER IN NEUTRON STARS

The neutron fluid region of a neutron star $[0.8\rho_0(0)<\rho<2\rho_0(0)]$ is expected to consist mainly of superfluid ($^3P_2$) neutrons with a small concentration of superconducting ($^1S_0$) protons and normal electrons [8]. These different particles are in beta equilibrium. The proton fraction $Y=Z/A$ can be evaluated minimizing the total energy per nucleon of nucleons and electrons,

$$B_{\rm tot}(\rho,Y)=B(\rho,Y)+\frac{Z}{A}m_pc^2+\frac{N}{A}m_nc^2+\frac{E_e}{A}\ , \tag{14}$$

with respect to Y. In Eq. (14), m_p and m_n are the proton and neutron rest masses and $B(\rho,Y)$ is the binding energy per nucleon for asymmetric nuclear matter. As we said in Sec II, it can be approximated, with a very good accuracy, by a quadratic dependence upon $\beta=(1-2Y)$ up to very high values of the asymmetry parameter. We assume that the electron energy E_e can be approximated by its relativistic free-gas expression. So we write

$$B(\rho,Y)+=B_0(\rho)+\beta^2E_{\rm sym}(\rho)\ , \tag{15}$$

$$\frac{E_e}{A}=c\sum_{p\sigma}(p^2+m^2c^2)^{1/2}\ , \tag{16}$$

where m is the electron mass and p its momentum. Electric charge neutrality implies that $Z=Z_e$ (i.e., $Y=Y_e$), and as a consequence, the proton Fermi momentum $k_F^{(p)}$ equals the electron Fermi momentum $k_F^{(e)}$. Using the ultrarelativistic limit of E_e, which is justified in the density range here considered, the proton fraction $Y(\rho)$ is the solution of the equation.

$$\frac{dB_{\rm tot}}{dY}=-4E_{\rm sym}(\rho)(1-2Y)+(m_p-m_n)c^2 +\hbar c(3\pi^2\rho)^{1/3}Y^{1/3} =0\ . \tag{17}$$

The results are reported in Table IV. In Ref. [28], where the superfluidity in a neutron star is extensively studied, it is shown that just in this range of Y values the peak of the gap of a proton superfluid occurs. In that reference a comparison with other calculations of the proton fraction is made. In Fig. 7 the effective mass of protons and neutrons in beta equilibrium are reported. They have been computed from the BHF self-consistent procedure for each Y previously determined according the Eq. (17). It is worth noting that the proton effective mass is much more suppressed compared to the neutron one since, as we saw in Sec. II, the proton mean field is much deeper for very asymmetric nuclear matter as an effect of the dominance of the p-n interaction. This feature, illustrated in Fig. 7, has an important implication in superfluidity. In fact, a smaller effective mass reduces the proton gap in the channel $^1S_0$ in comparison with the neutron gap in the same channel. Nevertheless, the proton component of superfluidity in a neutron star is still relevant.

TABLE IV. Proton concentration of nuclear matter in beta equilibrium versus the total baryon density. The values of the third column are obtained from Eq. (17) using the symmetry energy reported in Ref. [14]. The values of the fourth column have been given by A. Fabrocini (private communication).

	$10^2(Z/A)$		
ρ	Paris	Paris+3BF	UV14+UVII
0.038	2.75		
0.076	2.80	1.72	2.04
0.11	3.09	2.46	2.72
0.14	3.48	3.09	3.26
0.17	3.70	3.71	3.76
0.2	4.10	4.20	4.22
0.3	4.90	5.50	5.16
0.4	5.79		5.76

It has been assumed that the presence of electrons in a beta-equilibrium state of a neutron star could slightly modify the EOS [29]. A simple estimate of the correction can be given using an approximate solution of the equilibrium condition [Eq. (17)], which is

$$Y_{\rm eq}=\frac{1}{2}\left[\frac{4E_{\rm sym}}{\hbar ck_F}\right]^3\ . \tag{18}$$

This is a quite good approximation at high density where the effect we are studying is expected to be appreciable.

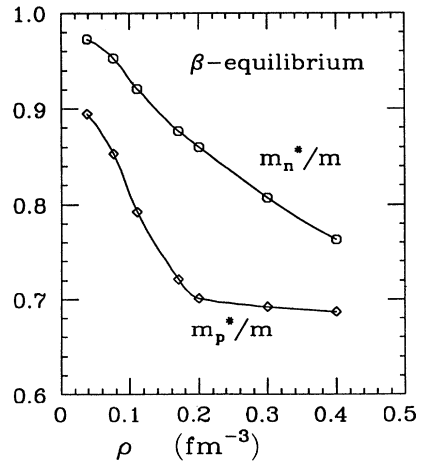

FIG. 7. Proton and neutron effective masses [Eq. (10)] versus total density for nuclear matter at beta equilibrium.

In this case the total energy per baryon can be written at the minimum,

$$B(\rho, Y_{eq}) - B(\rho, 0) = Y_{eq}(1-2Y_{eq})E_{sym} + (m_n - m_p)(1-Y_{eq}) . \quad (19)$$

For the higher value of density obtained ($\rho = 0.4$ fm^{-3}), the symmetry energy is 48.72 MeV and the electron (or proton) fraction is $Y_{eq} = 0.058$. We find then a correction to the EOS of 2.9 MeV, which amounts to $\sim 10\%$ of the pure neutron matter binding energy.

VI. CONCLUSIONS

The study of the EOS of asymmetric nuclear matter has been, in the last few years, a subject of renewed interest, particularly, in connection with astrophysical problems such as the understanding of the iron-core collapse of massive stars which produces type-II supernovae and the structure of the neutron-star remnants. The equation of state of neutron stars samples a range of densities and isospin asymmetry which is different from supernovae. Thus these two physical systems give the possibility of obtaining related but not identical information about the EOS.

The controversy over whether the EOS is "stiff" or "soft" is still unresolved. An aspect of this controversy is to understand whether or not the strongly asymmetric matter involved in a collapsing star could reduce the incompressibility or the energy of the electrons, in equilibrium with protons and neutrons, which could significantly affect the EOS. High-energy heavy-ion reactions indicated that the flow angle [30] and transverse momentum distribution [30,31] could be interpreted by assuming a stiff EOS. However, the observed data can be reproduced in microscopic Boltzmann-Uehling-Uhlenbeck calculations [32] using a softer EOS, when the momentum dependence of the mean field is properly taken into account [32,6]. Indeed, with a proper prescription on the momentum dependence, the mean field becomes less attractive at higher momenta and then it can simulate a stiff EOS.

A second question is whether the relaxation of the glitches observed in radio pulsars can be explained in terms of a viscous process of normal matter or whether it is evidence of superfluid matter inside neutron stars. Even in this case asymmetric matter properties are invoked to investigate the setting of proton superfluidity on the neutron background.

Quantitative estimates of the asymmetry in nuclear matter are based on the well-known phenomenological laws or, in the microscopic models, extrapolating the data taken from the two extreme situations of symmetric matter and pure neutron matter.

In this paper we have presented fully microscopic calculations. These enabled us to check the validity of phenomenological laws on the binding energy and neutron and proton mean fields. The BHF approximation to the Brueckner-Bethe-Goldstone theory is particularly suitable for obtaining greater physical insight into the problem. We found that the asymmetric matter binding energy as microscopically determined is in good agreement with the mass formula prediction. Its variation with neutron excess is mainly controlled by the tensor component of the *NN* interaction. The proton and neutron potentials exhibit a linear variation as a function of the asymmetry parameter, in agreement with recent investigations on the experimental proton and neutron Fermi energy in finite nuclei [26]. An appreciable deviation from symmetric change is observed as far as highly asymmetric matter is concerned.

The incompressibility strongly changes with the asymmetry parameter and exhibits a 30% of reduction when the supernova asymmetry ratio reaches a value of about 0.33 before collapsing. But the absolute magnitude of $K_0(0.33)$ depends on its value at the saturation point, which even in BHF approximation is not reliable.

The influence of the beta equilibrium becomes more and more important with increasing barion density, with the effect of softening the EOS. Moreover, for a density corresponding to the inner crust of a neutron star, we found a proton phase whose values of density and effective mass give a contribution to the $^1S_0$ superfluidity comparable to the neutron one.

ACKNOWLEDGMENTS

We thank M. Baldo, J. Cugnon, and A. Lejeune for valuable discussions and a critical reading of the manuscript. We thank also A. Fabrocini for providing us with some unpublished results on the proton contaminant.

*Electronic address: bombaci@catania.infn.it.
†Electronic address: lombardo@catania.infn.it.

[1] E. Baron, J. Cooperstein, and S. Kahana, Phys. Rev. Lett. **55**, 126 (1985).
[2] J. P. Blaizot, D. Gogny, and B. Grammaticos, Nucl. Phys. **A265**, 315 (1976); J. P. Blaizot, Phys. Rep. **64**, 171 (1980).
[3] S. H. Kahana, Annu. Rev. Nucl. Part. Sci. **39**, 231 (1989).
[4] N. K. Glendenning, Phys. Rev. Lett. **57**, 1120 (1986).
[5] R. Stock *et al.*, Phys. Rev. Lett. **49**, 1236 (1982); J. J. Molitoris, D. Hahn, and H. Stöcker, Nucl. Phys. **A447**, 13c (1985).
[6] J. Aichelin, A. Rosenhauer, G. Peilert, H. Stöcker, and W. Greiner, Phys. Rev. Lett. **58**, 1826 (1987); C. Gale, G. Bertsch, and S. Das Gupta, Phys. Rev. C **35**, 1666 (1987).
[7] M. Baldo, J. Cugnon, A. Lejeune, and U. Lombardo, Nucl. Phys. **A515**, 409 (1990), and references quoted therein.
[8] D. Pines and M. A. Alpar, Nature **316**, 27 (1985).
[9] J. Nemeth and D. W. L. Sprung, Phys. Rev. **176**, 1496 (1968); N. C. Chao, J. W. Clark, and C. H. Yang, Nucl. Phys. **A179**, 320 (1972).
[10] K. A. Brueckner, S. A. Coon, and J. Dabrowski, Phys. Rev. **168**, 1184 (1968); P. J. Siemens, Nucl. Phys. **A141**, 225 (1970).

[11] I. E. Lagaris and V. R. Pandharipande, Nucl. Phys. **A359**, 331 (1981).
[12] B. ter Haar and R. Malfliet, Phys. Rev. Lett. **59**, 1652 (1987).
[13] M. Prakash and T. L. Ainsworth, Phys. Rev. C **36**, 346 (1987).
[14] J. Cugnon, P. Deneye, and A. Lejeune, Z. Phys. A **328**, 409 (1987).
[15] R. B. Wiringa, V. Fiks, and A. Fabrocini, Phys. Rev. C **38**, 1010 (1988).
[16] B. D. Day, Rev. Mod. Phys. **39**, 719 (1967).
[17] M. Baldo, I. Bombaci, L. S. Ferreira, G. Giansiracusa, and U. Lombardo, Phys. Lett. B **209**, 135 (1988).
[18] M. Baldo, I. Bombaci, L. S. Ferreira, G. Giansiracusa, and U. Lombardo, Phys. Rev. C **43**, 2605 (1991).
[19] J. P. Jeukenne, A. Lejeune, and C. Mahaux, Phys. Rep. C **25**, 83 (1976).
[20] M. Baldo, I. Bombaci, G. Giansiracusa, U. Lombardo, C. Mahaux, and R. Sartor, Phys. Rev. C **41**, 1748 (1990).
[21] M. Baldo, I. Bombaci, G. Giansiracusa, and U. Lombardo, J. Phys. G **16**, L263 (1990).
[22] J. Haidenbauer and W. Plessas, Phys. Rev. C **30**, 1822 (1984); **32**, 1424 (1985).
[23] W. D. Myers and W. J. Swiatecki, Ann. Phys. (N.Y.) **55**, 186 (1969).
[24] M. Baldo, I. Bombaci, G. Giansiracusa, and U. Lombardo, Nucl. Phys. **A530**, 135 (1991).
[25] A. M. Lane, Nucl. Phys. **35**, 676 (1962).
[26] J. P. Jeukenne, C. Mahaux, and R. Sartor, Phys. Rev. C **43**, 2211 (1991).
[27] K. Kolehmainen, M. Prakash, J. M. Lattimer, and J. Treiner, Nucl. Phys. **A439**, 535 (1985).
[28] M. Baldo, J. Cugnon, A. Lejeune, and U. Lombardo, Nucl. Phys. (to be published).
[29] J. Cooperstein, Phys. Rev. C **37**, 786 (1988).
[30] H. A. Gustafsson *et al.*, Phys. Rev. Lett. **52**, 1590 (1984).
[31] P. Danielewicz and G. Odyniec, Phys. Lett. **157B**, 146 (1985).
[32] G. F. Bertsch and S. Das Gupta, Phys. Rep. **160**, 189 (1988).